

Article

# Biodiesel Production over Banana Peel Biochar as a Sustainable Catalyst

Ana Paula Soares Dias <sup>1,2,\*</sup> , Igor Pedra <sup>3</sup> , Érica Salvador <sup>3</sup> , Bruna Rijo <sup>2</sup>, Manuel Francisco Costa Pereira <sup>1</sup> ,  
Fátima Serralha <sup>3</sup>  and Isabel Nogueira <sup>4</sup> 

<sup>1</sup> CERENA, Instituto Superior Técnico, Universidade de Lisboa, Av. Rovisco Pais, 1, 1049-001 Lisboa, Portugal; mfcpc@tecnico.ulisboa.pt

<sup>2</sup> VALORIZA—Research Centre for Endogenous Resource Valorization, Instituto Politécnico de Portalegre, 7300-555 Portalegre, Portugal; bruna.rijo@ippportalegre.pt

<sup>3</sup> Escola Superior de Tecnologia do Barreiro, Instituto Politécnico de Setúbal, Rua Américo da Silva Marinho, 2839-001 Lavradio, Portugal; igor\_pedra99@sapo.pt (I.P.); ericasalvador.es@gmail.com (É.S.); maria.serralha@estbarreiro.ips.pt (F.S.)

<sup>4</sup> MicroLab, Instituto Superior Técnico, Universidade de Lisboa, Av. Rovisco Pais, 1049-001 Lisboa, Portugal; isabel.nogueira@tecnico.ulisboa.pt

\* Correspondence: apsoares@tecnico.ulisboa.pt

**Abstract:** Biodiesel from waste frying oil was produced via methanolysis using biochar-based catalysts prepared by carbonizing banana peels (350 °C and 400 °C) mixed with 20% (wt.) of alkali carbonates (Na, Li, or K). The catalysts exhibited a bi-functional character: acidic and basic. Raman spectroscopy confirmed the alkali's role in char graphitization, influencing morphology and oxygen content. Oxygenated surface sites acted as acidic sites for free fatty acid esterification, while alkali sites facilitated triglyceride transesterification. The best catalyst obtained by carbonization at 350 °C, without alkali modifier, led to 97.5% FAME by processing a waste frying oil with 1.2 mg KOH/g oil acidity. Most of the studied catalysts yielded high-quality glycerin, allowing the significance of homogenous catalyzed processes to be discarded.

**Keywords:** banana peel biochar; carbonization; bi-functional catalysts; biodiesel; transesterification; esterification



**Citation:** Soares Dias, A.P.; Pedra, I.; Salvador, É.; Rijo, B.; Costa Pereira, M.F.; Serralha, F.; Nogueira, I.

Biodiesel Production over Banana Peel Biochar as a Sustainable Catalyst.

*Catalysts* **2024**, *14*, 266. <https://doi.org/10.3390/catal14040266>

Academic Editors: Diego Luna and Guido Busca

Received: 26 February 2024

Revised: 26 March 2024

Accepted: 4 April 2024

Published: 16 April 2024



**Copyright:** © 2024 by the authors. Licensee MDPI, Basel, Switzerland. This article is an open access article distributed under the terms and conditions of the Creative Commons Attribution (CC BY) license (<https://creativecommons.org/licenses/by/4.0/>).

## 1. Introduction

The sustainability of planet Earth requires a drastic change in living standards to mitigate climate change induced by anthropogenic carbon emissions. The replacement of fossil fuels with renewable analogs is mandatory. Biodiesel produced by the alcoholysis of non-edible oils and fats is identified as a viable alternative to fossil-based diesel. Biodiesel is currently blended with fossil diesel to reduce the carbon footprint of land transport. The production cost of biodiesel is higher than that of fossil diesel [1], so many researchers have dedicated their work to investigating more sustainable production processes [2]. The replacement of the homogeneous catalyst currently used in the biodiesel industry with heterogeneous catalysts is pointed out as a way to increase the sustainability of biodiesel by reducing its production cost [3]. The raw materials used in biodiesel manufacturing, as well as the catalysts used, have a substantial influence on the sustainability of the produced biodiesel [4,5].

Biomass-based catalysts for biodiesel production have received a lot of attention from researchers since they can be produced from low-value residues and present meaningful catalytic capabilities [6]. The literature reports two types of biomass-based catalysts: ash-based catalysts that use the inorganic components of biomass and activated carbon-based catalysts (inorganics plus carbon-rich materials) [7].

Biochar-based catalysts, derived from biomaterials, have received much attention in the field of biofuel production for being easy to prepare and for presenting characteristics

relevant to good catalytic performances, such as a high specific area and high porosity, and for having functional groups on their surface which allow the tailoring of their properties [8]. Sustainable carbon materials with appealing catalytic performances can be prepared from biomass wastes using a few steps, being the methodologies schematized in Figure 1 [9].

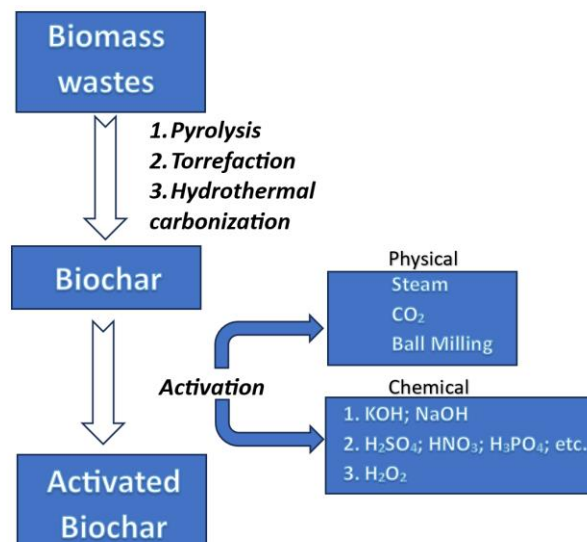


**Figure 1.** Preparation scheme of biochar-based catalysts (adapted from [9]).

According to a recent literature overview, the best method for producing biochar is slow pyrolysis [10]. To produce carbonaceous materials from the biomass, other, advanced techniques can be used: laser- and microwave-assisted carbonization [11]. The properties of the biochars depend on the raw biomass that was used to prepare them. The characteristics of the biochars are significantly influenced by the inorganic components of the biomass (K, Na, Ca, Mg, Fe, P, Si, and S) [12]. Their concentration rises throughout the charring process, and some of them can be transformed into oxides. K, Na, Ca, and Mg oxides give biochar its basic nature, whereas the P, Si, and S elements and the formation of oxygen functional groups (-COOH) provide biochar their acidic nature [12]. After being produced, biocarbon can undergo chemical and physical treatments to adjust its characteristics to improve its performance [13]. Alkali carbonates, such as  $K_2CO_3$ , were recently reported to be effective in increasing the surface area of banana peel biochar when used in the post-production activation procedure. The authors underlined the fact that  $K_2CO_3$  is an easier product to handle than the usual KOH used for the same purpose [14].

The biochar usually has an acidic character due to the surface functional groups that include heteroatoms such as oxygen, nitrogen, sulfur, and hydrogen. Thus, they are suitable for biodiesel production by esterification since transesterification by acid catalysis requires drastic reaction conditions with high temperature and pressure [15]. To be used in transesterification reactions, biochars have to undergo chemical/physical modifications or/and take advantage of some characteristics of raw biomass, such as high contents of alkaline and alkaline earth elements, which give them specific characteristics. Recently, Yameen et al. [13] reported the use of seaweed biomass to produce biochar catalysts for biodiesel production by transesterification. The authors mention that inorganics in raw biomass (Ca, K, Mg, and Fe, among others) in parallel with chemical and physical treatments play a crucial role in the catalytic performances. Foroutan et al. [16] also reported an excellent transesterification catalytic activity and stability of biochar catalysts modified with  $CaO/K_2CO_3$ . The researchers obtained a FAME yield of 98.83%, from waste frying oil, with a yield decay lower than 10% after the fourth reuse.

Bananas rank fourth in world food crops, which are headed by cereals: rice, wheat, and maize. The average yearly intake per person throughout the world is 12 kg, which results in a significant amount of banana peel waste (40% of the net weight of bananas). Banana peels (BP) contain compounds rich in carbon and a high content of inorganic elements (11.54%, dry basis) [17]. BP components such as cellulose, hemicellulose, and natural fibers can be converted into bioplastics, organic fertilizers, biofuels, and activated carbon which can be used as biofilters [18]. Other researchers used BP-activated carbon as an inexpensive and efficient electrode material [19]. Banana peel biochar, when applied as a soil amendment, shows superior environmental performances to raw banana peels [20]. An integrated approach to the energy valorization of banana peels was reported by Daimary et al. [21]. The researchers pyrolyzed banana peels for the production of bio-oil and biogas. The co-produced pyrochar was calcined to obtain an inorganic material rich in potassium salts which were used as a catalyst in the production of biodiesel by the methanolysis of waste frying oil. Unfortunately, the authors did not test pyrochar as a transesterification catalyst. Analogous catalysts were prepared by the calcination of a mixture of banana peels, roots, and trunks [22]. The obtained catalysts were successfully used in the production of biodiesel by the methanolysis of a mixture of vegetable oils. Jitjamnong et al. [23] prepared K-modified banana peel biochar catalysts for biodiesel production. The  $K_2CO_3$  salt was introduced by wet impregnation in a char post-production step. The best catalyst, prepared by pyrolysis at 600 °C, and 30%  $K_2CO_3$  allowed a FAME yield of 98.91%. The researcher underlined the fact that  $K_2CO_3$  improved the biochar's basicity. Higher alkali contents and pyrolysis temperatures had an almost null effect on basicity. The catalyst reuse test showed a fast catalytic activity decay which the author attributed to the intermediate washing procedure. After each reaction batch, the catalyst was washed with methanol and hexane followed by drying overnight at 105 °C. Mansoorsamaei et al. [24] recently described the production of banana peel biochar with magnetic properties driven by Fe species. The authors used low quality waste frying oil to evaluate the biochars catalysts in biodiesel synthesis, emphasizing that magnetic characteristics will allow for lower catalyst separation costs and emissions. Researchers also proposed a bi-functional reaction mechanism involving the adsorption of FFA over acid sites and methanol adsorption over basic sites.

Despite the extensive literature on biochar catalysts to produce biofuels like biodiesel, there is still more research to be done to improve their performance for industrial applications, notably in the field of their activation. According to Kumar et al. [25] the variability of the available biomass and the technology used in biochar production has to be analyzed from an economic point of view to scale up to large-scale production.

To contribute to the knowledge in the field of biomass-based catalysts, the following sections present results of the catalytic behavior in the oil methanolysis of biochars produced by banana peel carbonization using alkali carbonates (Na, Li, and K) as gasification catalysts.

## 2. Results and Discussion

The collected and dried banana peels were reduced to powder (<750 μm) and characterized by thermogravimetry to choose the carbonization temperature. The thermogram in Figure 2 shows a thermal degradation profile compatible with the composition given in the literature (Table 1). The main processes of weight loss (sugars, around 225 °C, hemicellulose with a shoulder around 275 °C, and cellulose around 330 °C) occur for temperatures lower than 400 °C. This observance led to the choice of 350 °C and 400 °C as carbonization temperatures, keeping in mind that the sustainability of the prepared catalysts requires a minimum energy consumption.

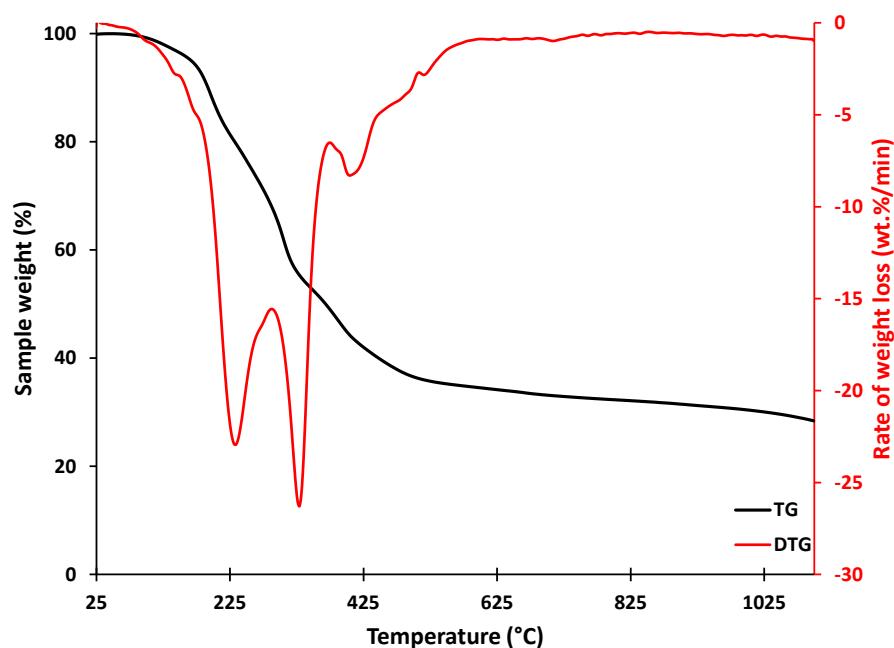


**Figure 2.** Thermogram, under  $N_2$  flow, of the dried banana peel ( $30\text{ }^\circ\text{C}/\text{min}$ ).

Alkali carbonates are reported as gasification catalysts, thus their presence will displace thermal degradation processes for lower temperatures [26]. Kobayashi and Kuramochi [27] recently observed a marked effect of  $K_2CO_3$  on the decrease of pyrolysis temperature for lignocellulosic mixed biomass. As a result, the alkali-doped chars were produced by carbonization at  $350\text{ }^\circ\text{C}$ .

**Table 1.** Banana peel composition (adapted from [28]). Ash composition values are averages from the literature.

	Weight (%)	Ash Composition	Weight (%)
Cellulose	12.2	K	20–40
Hemicellulose	10.2	Ca	10
Lignin (acid-detergent)	2.9	Mg	3–5
Sucrose	15.6	P	1–2
Glucose	7.5	Na	
Fructose	6.2	Fe	
Protein	5.1	Zn	Trace
Pectin	15.9	Mn	
Ash	9.8		

The obtained black and glazed chars were easily reduced to powder in a porcelain mortar. The morphology of the powdered chars was examined by SEM (Figure 3). The micrographs show clusters of irregular shapes and various sizes, with the largest in the hundred-micrometer range. The char produced at  $400\text{ }^\circ\text{C}$  shows smaller and more angular agglomerates than its counterpart produced at  $350\text{ }^\circ\text{C}$ , indicating that an increasing temperature makes the coal more fragile. The micrographs acquired at a higher magnification show that the larger agglomerates result from the sintering of smaller ones and emphasize the presence of little white grains owing to the alkalis. The appearance of the prepared chars, at  $350\text{ }^\circ\text{C}$  and  $400\text{ }^\circ\text{C}$ , seems less spongy than that reported in the literature for BP char obtained by more sophisticated techniques such as microwave-assisted carbonization [29]. Conventional pyrolysis at higher temperatures ( $600\text{ }^\circ\text{C}$ ) promotes chars with more compact morphologies than those in Figure 3 [30].

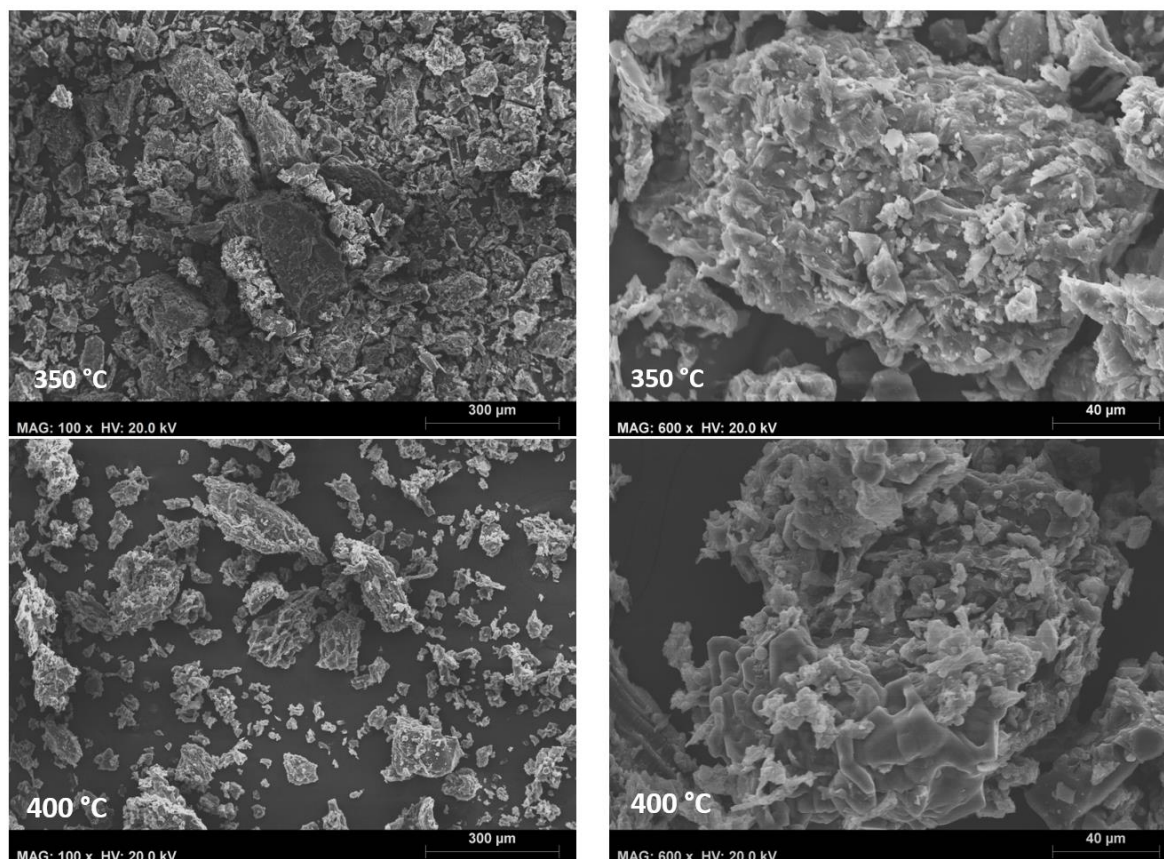


**Figure 3.** SEM micrographs of the fresh chars produced at 350 °C and 400 °C from raw banana peel.

The carbonization of BP added with alkali carbonates shows different morphologies from the biochars produced without the addition of alkali, Figure 4. The Li salt promoted a rounding of the agglomerates which have a less compact, more spongy appearance, which can be attributed to the role of the  $\text{Li}_2\text{CO}_3$  as a gasification catalyst [31]. The char produced with sodium carbonate had a more open morphology with the appearance of small overlapping flakes like that reported by Hu et al. [32] for BP char obtained by the molten-salts method. The char produced with potassium salt had a less open morphology since the gasification activity of alkali carbonates decreases with the element's atomic weight.

The EDS analysis (Figure 5) performed during SEM micrograph acquisition showed that chars are carbon-rich materials with C content above 60% (atomic) with oxygen content below 25% (atomic). As expected, with a rise in the carbonization temperature, the C content increased [33]. The char modified with alkali showed a slightly lower C content and higher oxygen content. The O content of the alkali-modified chars was in accordance with the catalytic behavior of the alkali carbonate described by Kapteijn et al. [34]. The carbonization temperature and the presence of alkali salts also influenced the near-surface K level, with potassium-modified char having the greatest K content. Potassium was the main inorganic element detected for unmodified chars, which agrees with the banana peel ash composition in Table 1.

The char modified with Na salt only presented with a small content of Na in near-surface layers (EDS analysis), meaning that this element was distributed in char bulk and thus inaccessible to catalyze homogeneous processes during the methanolysis reaction.

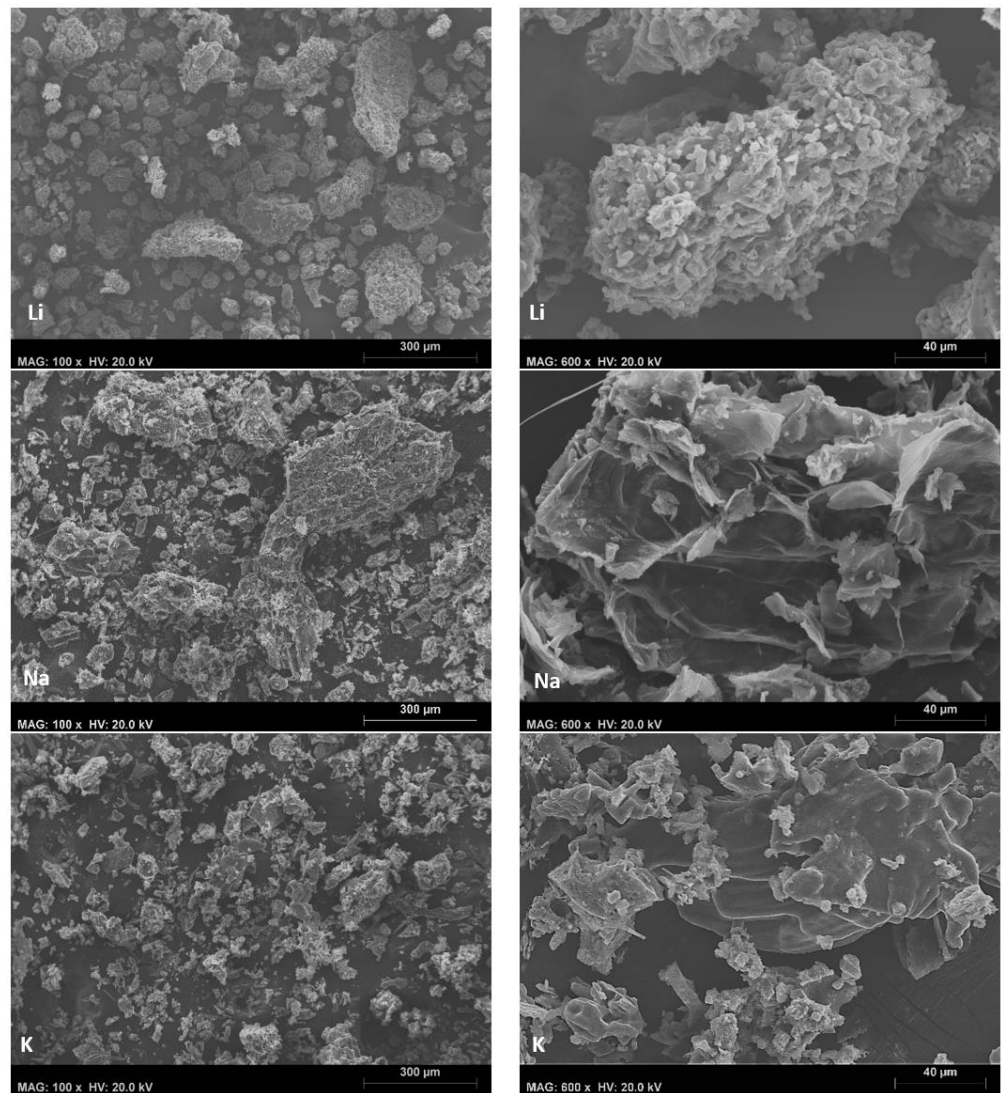


Figure 4. SEM micrographs of the fresh alkali-modified chars produced at 350 °C.

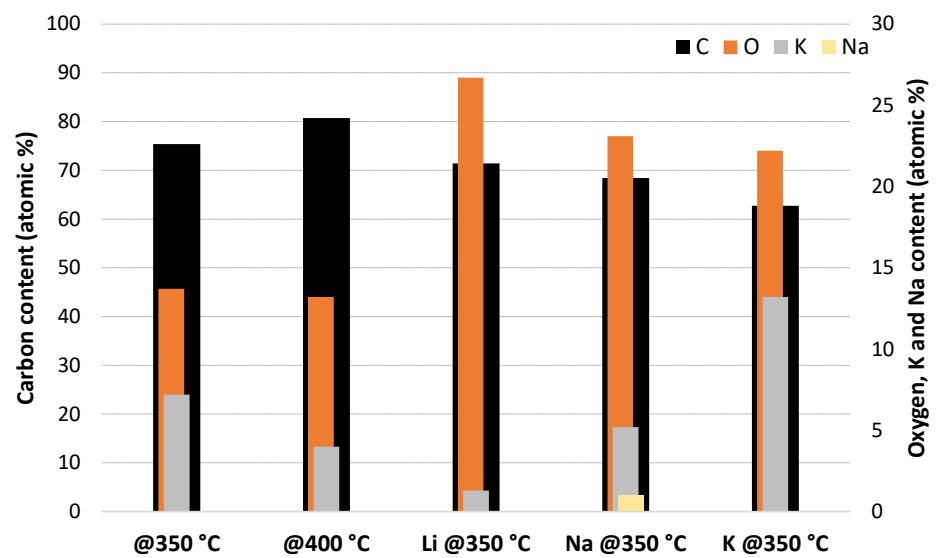


Figure 5. Carbon, oxygen, and potassium atomic contents, by EDS, of the as-prepared chars.

The powders were characterized by X-ray diffraction to assess graphitization and the presence of crystalline phases derived from biomass ash and alkalis introduced as carbonate salts. The diffractograms in Figure 6 show that sylvite (KCl) is the main crystalline phase for all of the samples, which is compatible with the fact that K can reach 78 g/kg of dried peel [34]. Potassium-containing salts (oxide, carbonate, and chloride) are the main crystalline phases in banana peel ash [35], which are obtained in the oxidative atmosphere, air, and at higher temperatures than those used to prepare chars. The catalysts modified with Na and Li carbonate showed XRD lines of alkali carbonates in addition to those of sylvite but the sample modified with  $K_2CO_3$  only presented with the lines of sylvite, which seems to be the result of well-dispersed nanocrystals of K carbonate in the biochar matrix. The post-reaction catalysts were also characterized by XRD. The diffractograms in Figure 7 show that post-reaction catalysts lose part of the crystalline KCl, making visible the XRD pattern of the carbonaceous material with a low degree of graphitization. According to Spataru et al. [36], the broad features centered around  $23^\circ$  and  $44^\circ$  are ascribable to graphitic planes (002) and (001). The authors underlined that broad lines indicate that chars have amorphous structures formed by disordered polycyclic aromatic carbon sheets with a low content of crystalline graphite. The sample prepared at  $400^\circ\text{C}$  showed higher stability than the one prepared at  $350^\circ\text{C}$ . The sample prepared at  $350^\circ\text{C}$  and in contact with methanol provided evidence, as reported before [37], that sylvite is soluble in methanol. The diffractogram of the biochar obtained by the carbonization of raw banana peel at  $350^\circ\text{C}$ , and subsequent methanol contact, confirmed the leaching of KCl by methanol. This aligns with published findings on sylvite's solubility in methanol [37]. The XRD patterns of the post-reaction catalysts doped with alkali carbonate (Figure 8) show that the diffraction lines of Na and Li carbonates overlapped, whereas the sample doped with K carbonate only presented with the diffractogram of the carbonaceous material. The low solubility of sodium carbonate in the oil transesterification reaction medium was stated by Rijo et al. [38]. The minor leaching of lithium carbonate is consistent with the findings of Dai et al. [39].

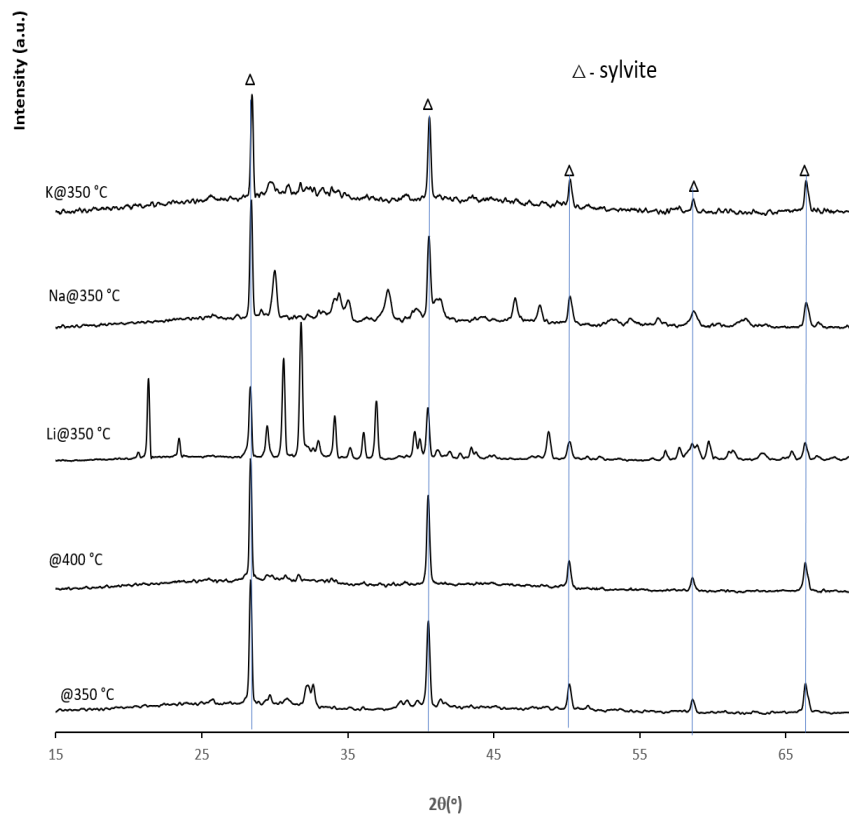
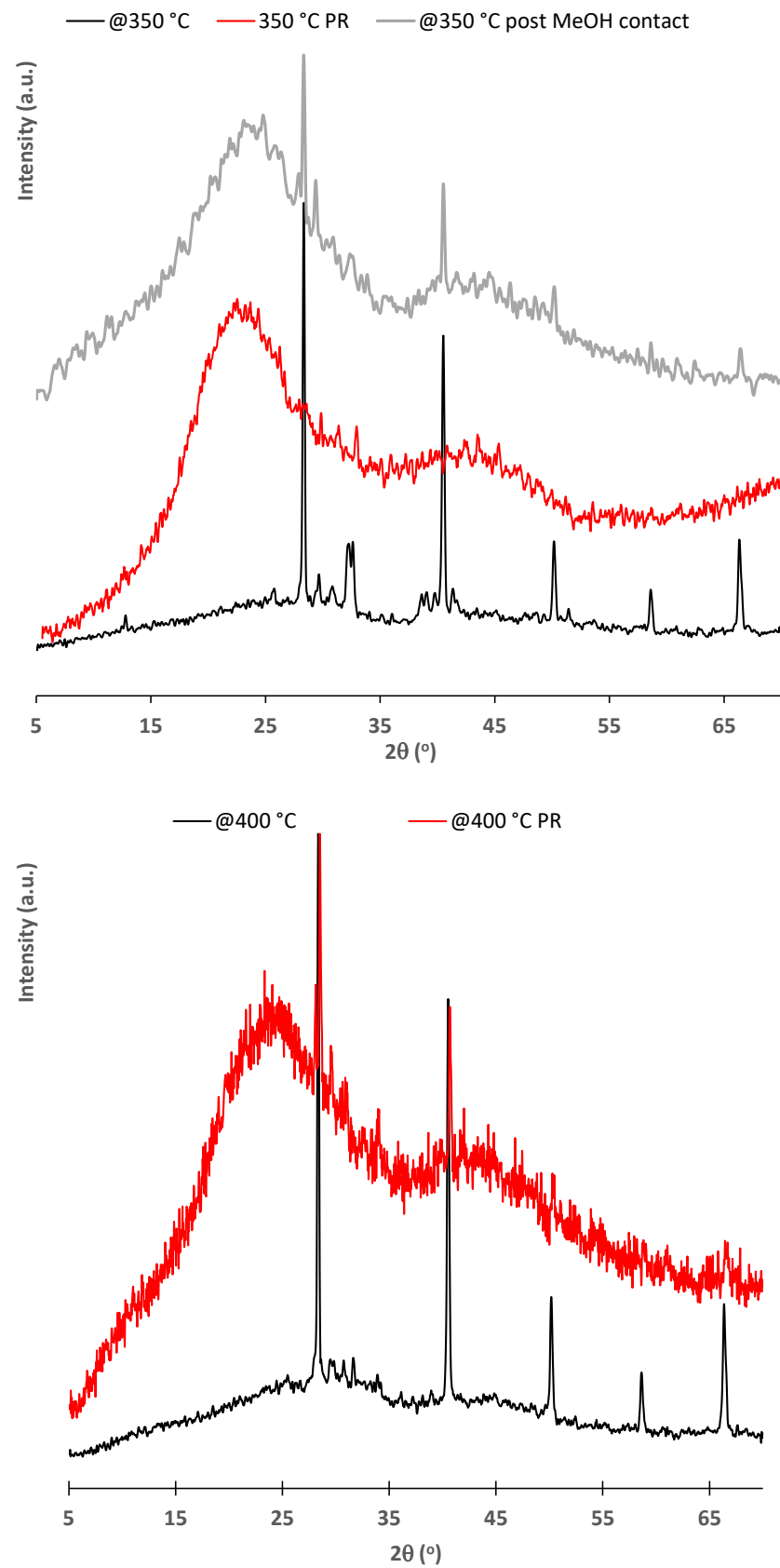


Figure 6. XRD patterns of fresh catalysts.



**Figure 7.** XRD patterns of fresh and post-reaction, and post methanol contact, catalysts without alkali modifiers.

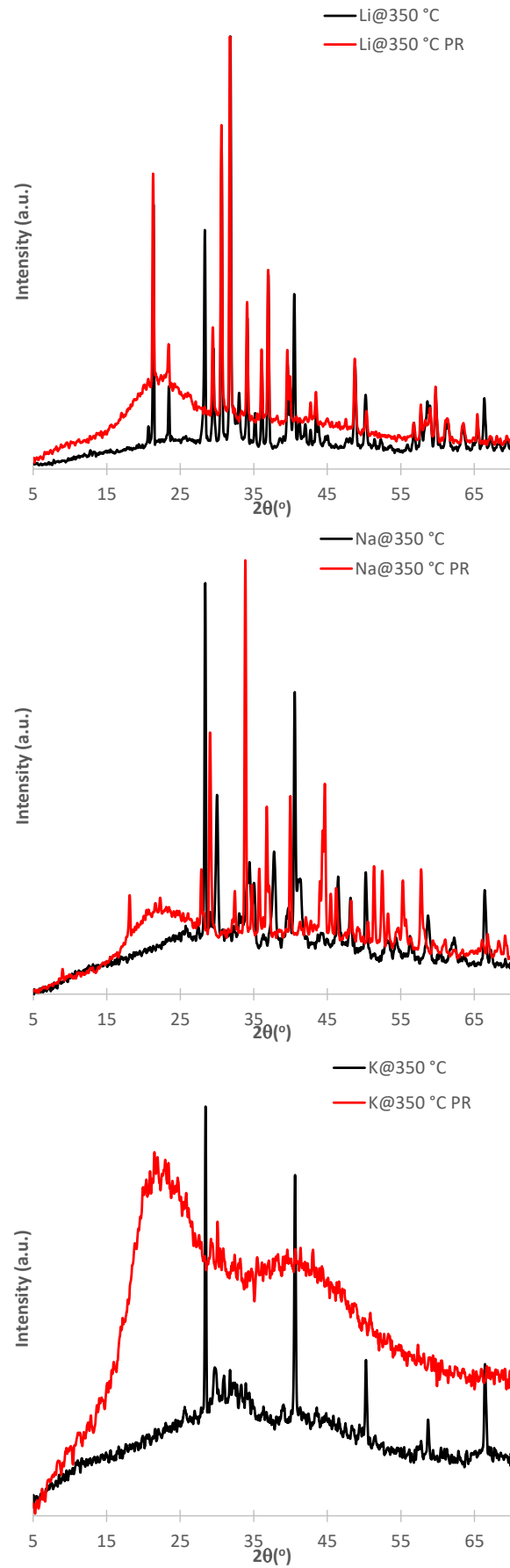
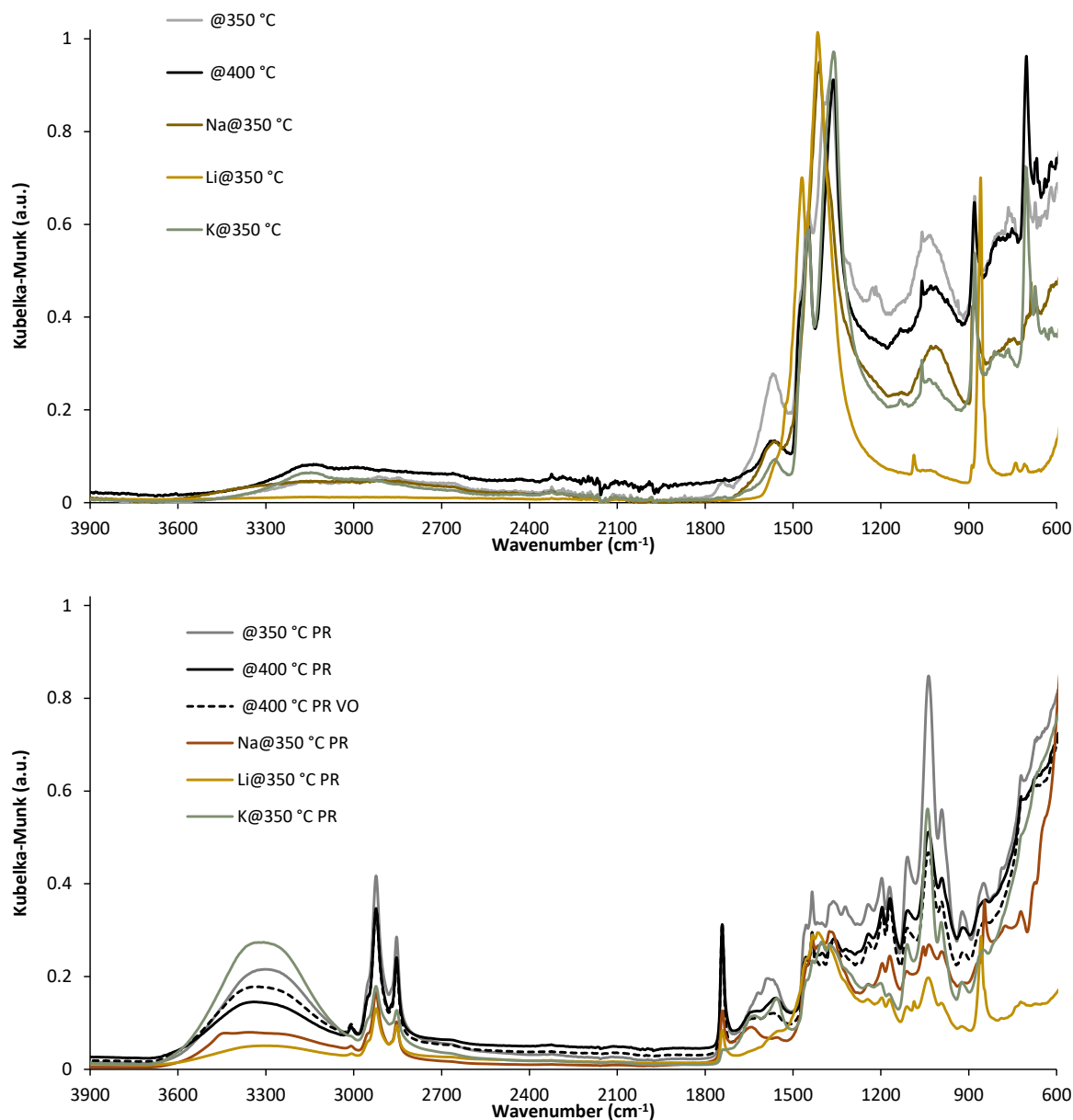


Figure 8. XRD patterns of fresh and post-reaction catalysts modified with alkali carbonate.

The FTIR spectra of fresh (Figure 9) catalysts present the main reflection bands in the 1500–1700  $\text{cm}^{-1}$  wavenumber range. The unmodified samples present two main bands centered at 1360  $\text{cm}^{-1}$  and 1465  $\text{cm}^{-1}$  ascribable to O-C-O and -C=O [40] species on the char surfaces. Data presented by Zeghioud et al. [40] show that alkali modifiers promote deviations of these bands, which justifies the complexity of the spectra of the chars with alkali additives. The broad band at 1046  $\text{cm}^{-1}$ , which is absent for the Li-modified char is attributed to C-O-C vibrations [41].



**Figure 9.** ATR-FTIR spectra of fresh and post-reaction catalysts.

The Li and Na-modified chars are dominated by the IR bands of inorganic additives. The unmodified char prepared at 350  $^{\circ}\text{C}$  presents an additional shoulder around 1400  $\text{cm}^{-1}$  belonging to -C-O vibration mode. The absence of these species for the other chars seems to point out that alkali modifiers and higher carbonization temperatures increase the deoxygenation of biomass [42]. Alkali modifiers also promote deacidification reactions, which is beneficial since transesterification reactions perform better with basic character catalysts. The unmodified char made at 350  $^{\circ}\text{C}$  presents an intense reflectance feature in the range 1400–1600  $\text{cm}^{-1}$  which can be attributed to -COO acidic species [43]. This sample

also presents a more intense band, than the other samples, around  $1558\text{ cm}^{-1}$  which is attributable to C=C of aromatics [43]. For all of the fresh samples, the spectral range above  $2900\text{ cm}^{-1}$  is almost flat, which indicates the absence of -OH hydroxyl ( $3445\text{ cm}^{-1}$ ) and -OH phenolics and alcohols ( $3630\text{ cm}^{-1}$ ) groups [41] on the surface of the char. All the post-reaction catalysts show IR bands typical of the reaction species. The appearance of the broad band centered around  $3300\text{ cm}^{-1}$  seems to indicate that methanol and glycerin are preferentially adsorbed by the catalysts. The spectra of biodiesel and oils (Figure S1 in the supplementary data section) clearly show the absence of such a band. The post-reaction biochar modified with K carbonate shows an intense band around  $1000\text{ cm}^{-1}$  which indicates glycerin adsorption [44]. Such a result is compatible with the fact that biochars are referred to as sorbents for the dry wash purification of biodiesel [45]. The unmodified char catalyst produced at  $400\text{ }^{\circ}\text{C}$  was evaluated for different methanol/oil ratios and catalyst/fat ratios to identify the optimal reaction conditions. Based on the results presented in Table 2, a higher FAME yield was produced with a 5 wt.% catalyst and a methanol/fat ratio of 15. Similar results were reported by Wang et al. [46] for K-modified biochar catalysts prepared by wet impregnation with the  $\text{K}_2\text{CO}_3$  of char obtained by the pyrolysis ( $600\text{ }^{\circ}\text{C}$ ) of peat. The authors reported that for catalyst loading larger than 5 (wt.%), the FAME yield remained almost constant, and the same was observed for MeOH/oil ratios higher than 8. The researchers observed K leaching but the catalysts showed residual catalytic activity due to stable Al-O-K species on the catalyst surface. Jitjamong et al. [23], using a Response Surface Optimization methodology, obtained an optimal FAME yield of 98.91% for an MeOH/oil = 15, a 4 wt.% of catalyst,  $65\text{ }^{\circ}\text{C}$ , and 120 min reaction time. Such results are slightly better than that of Table 2 but the catalyst was prepared in a more complex, thus less sustainable, procedure including a pyrolysis step at  $600\text{ }^{\circ}\text{C}$ , followed by KOH activation and then impregnation with an aqueous solution of  $\text{K}_2\text{CO}_3$ .

**Table 2.** Graphitization index ( $I_D/I_G$ ) and  $I_G/I_{\text{all}}$  Raman parameters of the as-prepared chars.

Char	@350 °C	@400 °C	Li@350 °C	Na@350 °C	K@350 °C
$I_D/I_G$	1.737	1.643	1.212	1.165	1.360
$I_G/I_{\text{all}}$	0.298	0.264	0.267	0.253	0.290

The Raman spectra in Figure 10 show the characteristic bands of biochar with the most intense centered at  $1350\text{--}1370\text{ cm}^{-1}$  and  $1580\text{--}1600\text{ cm}^{-1}$  attributed to  $\text{sp}^2$  vibrations of species with defects (D band) and graphitized species (G band), respectively [41]. The graphitization index ( $I_D/I_G$ ) and the  $I_G/I_{\text{all}}$  of the carbonized materials were computed and the values are summarized in Table 2. An increase in the carbonization temperature promotes a decrease in the valley band intensity (centered at  $1400\text{ cm}^{-1}$ ) due to the decrease in amorphous or defective carbon species, such as those containing oxygen. Also, the band centered around  $1200\text{ cm}^{-1}$  due to the small carbon ring species or C-H, C-O and C=O [47] decreases for char produced at higher temperature. The char produced with alkali carbonate catalysts shows distinct Raman spectra underlining the chief role of alkali in the carbonization process. The Li salt produced a char with a well-defined G band without the shoulder for lower wavenumbers indicating the absence of small ring and C-H, C-O and C=O species. The Na and K salts were less effective in the production of well-organized carbon material, which can be related to their relatively lower activities as gasification catalysts [48]. Data in Table 2 prove that higher carbonization temperature increases the graphitization index but alkali salts, at lower temperature, have the same effect. The relative intensity of the G band in the spectral range analyzed does not vary substantially (0.25–0.30) either with the carbonization temperature or with the presence of the alkaline salts, probably due to the relatively low range of carbonization temperatures used.

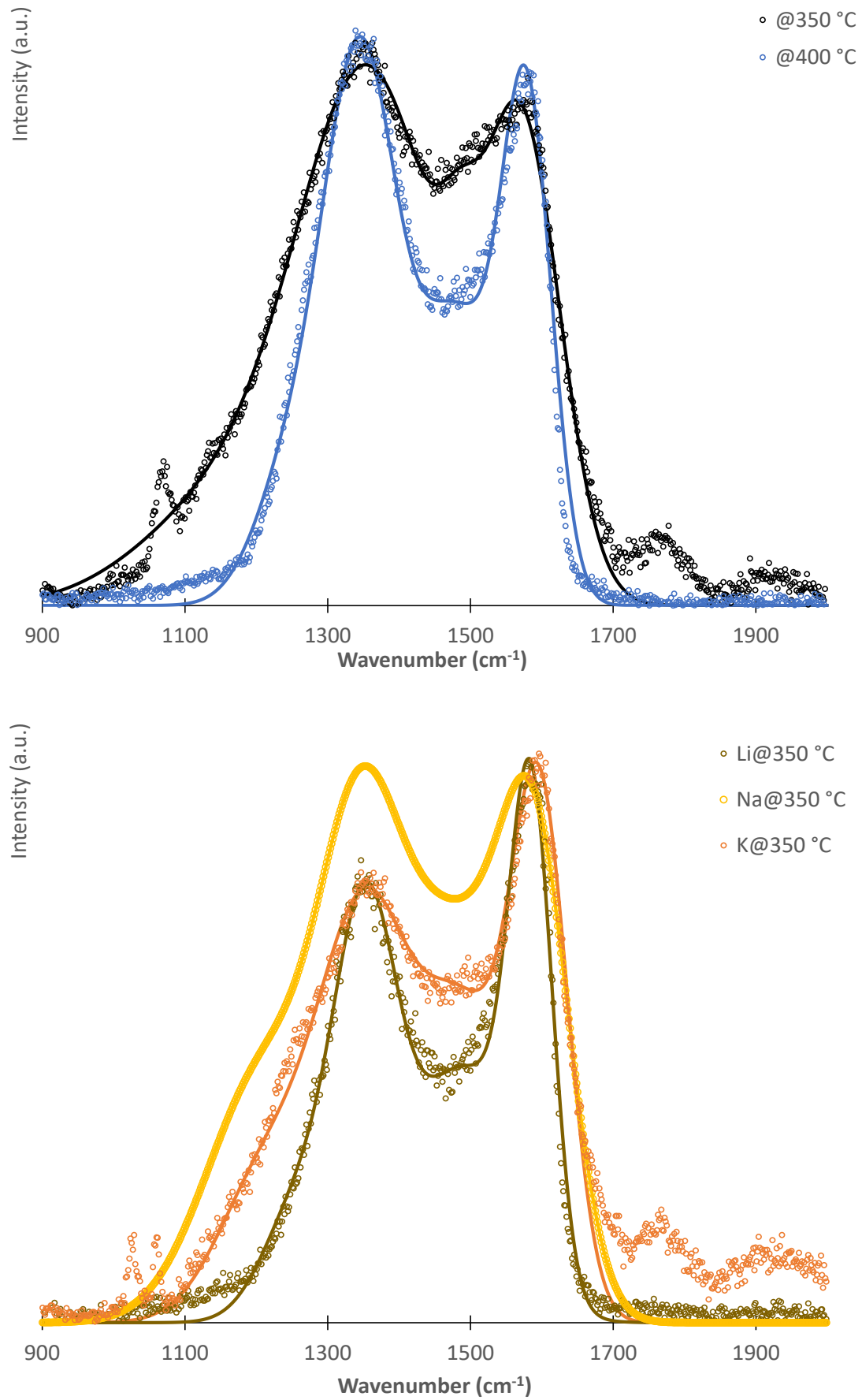


Figure 10. Raman spectra of the as-prepared chars.

The catalytic performances of the unmodified char produced at 400 °C was evaluated for different methanol oil ratios and catalyst/fat ratios to identify the optimal reaction conditions. Based on the results presented in Table 3, a higher FAME yield was produced with a 5 wt.% catalyst and a methanol/fat ratio of 15. Similar results were reported by Wang et al. [46] for K-modified biochar catalysts prepared by wet impregnation with  $K_2CO_3$  of char obtained by pyrolysis (600 °C) of peat. The authors reported that for catalyst loading larger than 5 (wt.%) the FAME yield remained almost constant, and the same was observed for MeOH/oil ratios higher than 8. The researchers observed K leaching but the catalysts showed residual catalytic activity due to stable Al-O-K species on the catalyst surface. Jitjamong et al. [23] using a Response Surface Optimization methodology obtained an optimal FAME yield of 98.91% for MeOH/oil = 15, 4 wt.% of catalyst, 65 °C, and 120 min of reaction. Such results are slightly better than that of Table 2 but the catalyst was prepared in a more complex thus less sustainable, procedure including a pyrolysis step at 600 °C, followed by KOH activation and then impregnated with an aqueous solution of  $K_2CO_3$ .

**Table 3.** FAME yield (wt.%) from WFO, obtained from different reaction conditions using unmodified char catalysts prepared at 400 °C.

	$W_{cat}/W_{fat}$ (wt. %)	MeOH/WFO (molar)	FAME (wt. %)
@400 °C WFO; 180 min	5	15	95.8
		12	91.0
		9	69.1
	7	12	91.8
		15	92.9
		9	92.3

The prepared biochar catalysts were tested in the methanolysis reaction of waste frying oil (acidity 1.2 mg<sub>KOH</sub>/g<sub>oil</sub>) and vegetable oil (acidity 0.34 mg<sub>KOH</sub>/g<sub>oil</sub>) was used as a reference.

Data in Figure 11 showed that the banana peel char catalyst, obtained at 400 °C, was slightly sensitive to the fat acidity since the vegetable oil in analogous conditions allowed a higher FAME yield (97.9% instead of 95.8%). Considering there was no formation of an intermediate layer between glycerol and FAME as predicted, the soap produced during the processing of WFO, which is more acidic than VO, appears to have been adsorbed on the catalyst. There was no difficulty in separating FAME and glycerin, as is expected when soap exists in the reaction mixture.

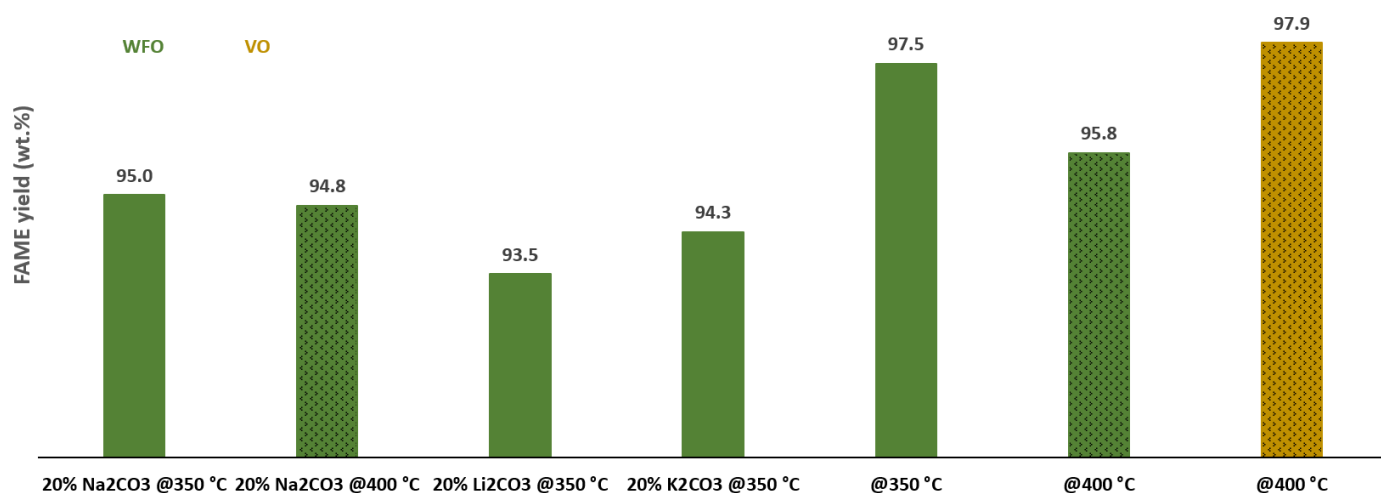


**Figure 11.** FAME yield (5 wt.%) obtained by transesterification at methanol reflux temperature, 5% wt. of catalyst, MeOH/fat = 15 molar ratio, 180 min.

The banana peel biochar obtained at 350 °C was more effective than its analogous biochar made at 400 °C. This observance could be due to its more acidic character since this catalyst showed intense IR bands belonging to -COOH species.

Thus, it can act as a bi-functional catalyst performing, simultaneously, the esterification, of free fatty acids and transesterification of triglycerides. All of the alkali-modified char catalysts display analogous catalytic behavior and have been less performant than the unmodified char because they present higher oxygen content (Figure 5), probably as acidic functional groups that are less active in transesterification reactions than basic active sites. The slight differences in the catalytic behavior of alkali-doped chars can be related to the different morphologies (Figure 4) presented. The Na-modified sample shows the most favorable morphology for the catalyst role. The alkali on the catalysts surfaces, clearly visible in the FTIR spectra of fresh catalysts, also has a chief role in the catalytic behavior. The biochar produced without an alkali modifier, which showed higher FAME yields, are those with the higher hydrophilic characteristics which present more intense -OH FTIR bands (Figure 10) for post-reaction samples.

The FAME yields obtained are in line with those reported in the literature for analogous catalytic systems. Recent reported data [24] showed slightly lower FAME yields (around 90%) which can be due to the fact that a lower catalyst loading (4% instead 5% wt.%) and methanol/oil ratio were used.

The FTIR analysis of the glycerin co-produced with FAME was used to determine their purity (MONG content, organic matter non-glycerin) [49,50] and the likely involvement of homogeneous catalytic processes. The spectra in Figure 12 are typical of glycerin produced via heterogeneous catalysis, which is similar to commercial glycerin [50]. Only the glycerin spectrum produced with K<sub>2</sub>CO<sub>3</sub>-doped char shows significant MONG contamination (IR features in the 1750–1150 cm<sup>-1</sup> range), suggesting the contribution of homogeneous catalysis [49] promoted by the leached K species. This finding is consistent with the X-ray diffractogram (Figure 8) of the post-reaction catalyst, which revealed the total removal of the sylvite diffraction lines. The high purity of the glycerol produced can also be attributed to the fact that the charcoal of the catalysts acts as a sorbent removing, in situ, species such as soaps eventually formed during methanolysis. The good purity of the glycerin produced can also be since the char catalysts work as sorbents, eliminating species such as soaps that are eventually generated during methanolysis. Recent unpublished findings suggest that chars produced by the carbonization of waste biomass are effective in biodiesel glycerin purification.

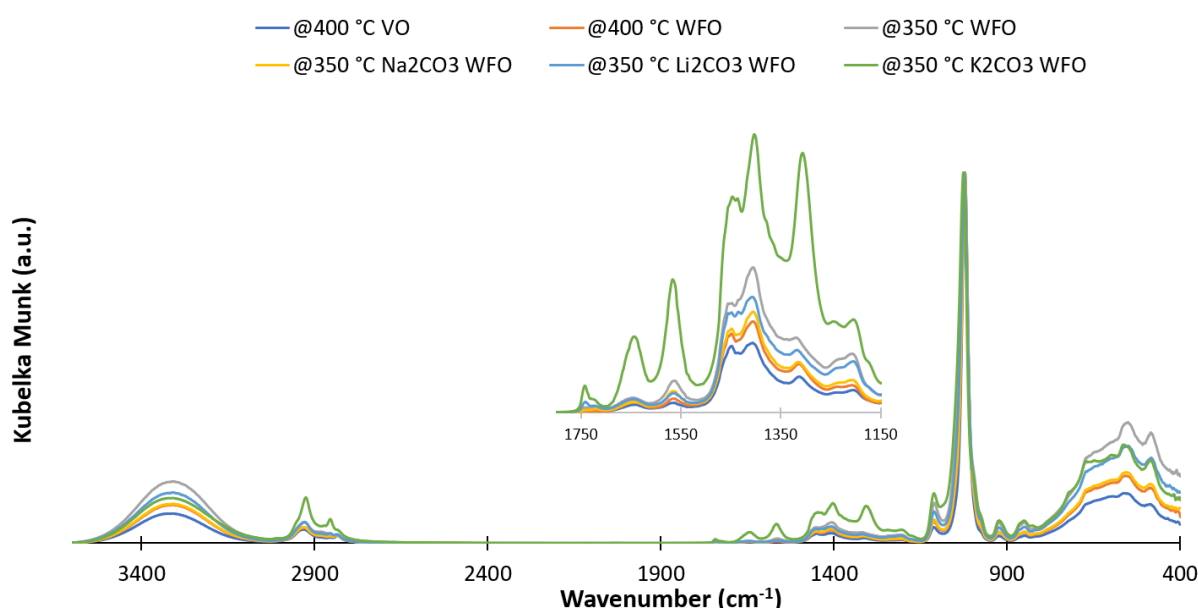


Figure 12. FTIR spectra of the co-produced glycerins.

### 3. Experimental Section

#### 3.1. Biochar Production and Characterization

The biochar catalysts were prepared by the carbonization of banana peels modified with alkali (Li, Na, and K) carbonate salts (20 wt.%). The banana peels from the household waste bin were dried overnight at 60 °C and powdered using a blade mixer. The biomass and alkaline carbonates were mixed and homogenized in a mechanical mortar and pestle for 10 min. A total of 10 g of the biomass/alkali mixtures were enclosed in an aluminum envelope, to minimize contact with the atmosphere inside the furnace, and carbonized in a muffle at 350 °C and 400 °C using a heating rate of 3 °C/min and with a residence time of 2h at maximum temperature. A small hole in the envelope allowed the gases formed during carbonization to escape. The carbonization temperature range was selected from the thermal degradation profile obtained by thermogravimetry under N<sub>2</sub> flow. The thermograms were acquired for 45–60 mg of powdered biomass (dried) in a Netzsch STA490 PC thermobalance using a 30 °C/min heating rate from 30 °C to 1100 °C. The morphology of the as-prepared biochar was evaluated by scanning electron microscopy (SEM). The micrographs were collected using a Joel JSM7001F FEG-SEM microscope, equipped with an energy dispersive X-ray spectroscopy (EDS) detector to quantify the elemental composition of the sample. The powdered biochar samples were previously studded over carbon adhesive disks, double-sided, and covered with a thin metallic film.

The degree of graphitization of the as-prepared chars was evaluated by Raman spectroscopy. The spectra were collected using a Horiba LabRam HR 800 Evolution confocal Raman micro spectrometer with a 532 nm laser focused with a 100× objective with 10 mW power at the samples. To calculate the degree of graphitization of the samples, the deconvolution method was applied to the spectral data in the 900–2000 cm<sup>-1</sup> range as reported before [51]. The I<sub>D</sub>/I<sub>G</sub> was obtained by the ratio of the areas under the Gaussian curves centered at 1367 cm<sup>-1</sup> (D band) and 1587 cm<sup>-1</sup> (G band). The ratio of the area of the G band to the total area of the spectrum in the analyzed wavenumber range was calculated and taken as a measure of the graphitization of the char [52]. The morphology of chars was evaluated by scanning electron microscopy (SEM). The micrographs were acquired for powdered samples dispersed over carbon adhesive tape covered with a thin film of metal. The fresh and post-reaction catalysts were characterized by XRD. The diffractograms were acquired from 5° to 70° on a Bruker D8 Advance Powder Diffractometer, with Cu K<sub>α</sub> radiation with a step of 0.02°/s. Fresh and post-reaction biochar catalysts were characterized by ATR-FTIR to infer the surface functional groups in fresh samples and the adsorption of reaction species for the used catalysts. The infrared spectra were acquired using an ATR-FTIR with a PerkinElmer Spectrum Two IR spectrometer, with a resolution of 4 cm<sup>-1</sup>, 4 scans, and a wavelength between 4000 cm<sup>-1</sup> and 600 cm<sup>-1</sup>. The ATR accessory, from Pike, was equipped with diamond crystal. To assess data reproducibility, all catalytic tests were performed in triplicate.

#### 3.2. Oil Methanolysis Catalytic Tests

Biodiesel was produced by transesterification of waste frying oil (WFO) from a local restaurant over biochar-based catalysts. The WFO was filtered before the reaction to remove solid contaminants from foods that had been fried. The catalytic tests were carried out at methanol (MeOH) reflux temperature, in a 3-neck round-bottom Pyrex flask equipped with a reflux column. Each catalytic test was performed using 50 g of WFO with a MeOH/oil molar ratio of 9–15 and 5%, or 7%, of solid catalyst (oil basis) for 180 min. Vegetable oil (VO, alimentary grade) was used as a standard for the catalytic behavior. As described before [38], the acidity of the VO and WFO were accessed by titration with KOH using phenolphthalein (ethanol solution) as a colorimetric indicator. The methanol was previously contacted with a solid catalyst for 30 min and then the pre-heated (67 °C) oil was added to start the time counting. After the reaction period the catalyst was removed by filtration and the liquid mixture was placed in a funnel for the gravitational separation of the formed glycerol from the methyl esters and the unreacted oil. The FAME and the glycerin

containing liquids were characterized by ATR-FTIR as reported before [38]. The FAME content was computed considering the area of the band centered at  $1436\text{ cm}^{-1}$  and the spectral area in the range of  $1480\text{--}1410\text{ cm}^{-1}$ . A calibration curve was obtained analyzing FAME/WFO mixtures with FAME content in the 100–75% range (data in supplementary data section). For the calibration curve, FAME was obtained by WFO transesterification using NaOH catalyst precursor and classic purification with  $\text{H}_2\text{SO}_4$  aqueous solution [44]. IR spectra were plotted under the conditions described in the above Section 3.1.

#### 4. Conclusions

Food waste such as banana peels can be used to prepare carbon-rich materials with interesting catalytic properties in biodiesel production by transesterification. The carbonization of banana peels leads to the formation of biochar with trapped inorganic material (ashes, mainly KCl), which gives it a basic character and activity in the methanolysis of oils for biodiesel production. As the biochar produced at a low temperature ( $350\text{ }^\circ\text{C}$ ) has acidic functional groups on its surface, it can catalyze both esterification and transesterification reactions. The bi-functional character (acidic and basic) of the biochar makes it suitable for processing oils with considerable acidity such as waste frying oils. As reported in the literature, potassium is leached into the reaction medium as it is soluble in methanol. The carbonization of banana peels in the presence of Na, Li, and K carbonates leads to the formation of basic character biochars with catalytic activity similar to unmodified biochar, but the removal of acidic functional groups reduces their esterification activity. Na and Li alkali have a lower leaching rate than K. The biochars, which constitute part of the catalyst mass, also act as sorbents for the species in the reaction medium, which leads to the production of high-purity glycerin.

**Supplementary Materials:** The following supporting information can be downloaded at: <https://www.mdpi.com/article/10.3390/catal14040266/s1>, Figure S1: FTIR of FAME (purified), WFO and VO.

**Author Contributions:** A.P.S.D.: Conceptualization, Resources, Supervision, Writing—review & editing; I.P.: Investigation, Writing—original draft; É.S.: Investigation; Writing—original draft; B.R.: Methodology, Writing—review & editing; M.F.C.P.: Investigation, Formal analysis, Resources; F.S.: Supervision; I.N.: Investigation, Formal analysis. All authors have read and agreed to the published version of the manuscript.

**Funding:** This work was partially supported through FCT strategic funding of CERENA (UIDB/04028/2020).

**Data Availability Statement:** Data will be made available on request.

**Acknowledgments:** The authors would like to thank the Fundação para a Ciência e a Tecnologia for partially funding this work through the CERENA project, under project UIDB/04028/2020.

**Conflicts of Interest:** All authors declare that they have no conflicts of interest.

#### References

1. Biodiesel and Diesel Prices, 2019 to April 2022—Charts—Data & Statistics—IEA, (n.d.). Available online: <https://www.iea.org/data-and-statistics/charts/biodiesel-and-diesel-prices-2019-to-april-2022> (accessed on 31 July 2023).
2. Esmaeili, H. A critical review on the economic aspects and life cycle assessment of biodiesel production using heterogeneous nanocatalysts. *Fuel Process. Technol.* **2022**, *230*, 107224. [CrossRef]
3. Maleki, B.; Talesh, S.A.; Mansouri, M. Comparison of catalysts types performance in the generation of sustainable biodiesel via transesterification of various oil sources: A review study. *Mater. Today Sustain.* **2022**, *18*, 100157. [CrossRef]
4. Riaz, I.; Shafiq, I.; Jamil, F.; Al-Muhtaseb, A.H.; Akhter, P.; Shafique, S.; Park, Y.-K.; Hussain, M. A review on catalysts of biodiesel (methyl esters) production. *Catal. Rev.* **2022**, *11*, 1–53. [CrossRef]
5. Bashir, M.A.; Wu, S.; Zhu, J.; Krosuri, A.; Khan, M.U.; Aka, R.J.N. Recent development of advanced processing technologies for biodiesel production: A critical review. *Fuel Process. Technol.* **2022**, *227*, 107120. [CrossRef]
6. Pan, H.; Xia, Q.; Wang, Y.; Shen, Z.; Huang, H.; Ge, Z.; Li, X.; He, J.; Wang, X.; Li, L.; et al. Recent advances in biodiesel production using functional carbon materials as acid/base catalysts. *Fuel Process. Technol.* **2022**, *237*, 107421. [CrossRef]

7. Changmai, B.; Vanlalveni, C.; Ingle, A.P.; Bhagat, R.; Rokhum, S.L. Widely used catalysts in biodiesel production: A review. *RSC Adv.* **2020**, *10*, 41625–41679. [[CrossRef](#)] [[PubMed](#)]
8. Lee, J.; Kim, K.H.; Kwon, E.E.; Bhatia, S.K.; Palai, A.K.; Kumar, A.; Bhatia, R.K.; Patel, A.K.; Thakur, V.K.; Yang, Y.H. Trends in renewable energy production employing biomass-based biochar. *Renew. Sustain. Energy Rev.* **2017**, *77*, 125644. [[CrossRef](#)]
9. Parida, S.; Singh, M.; Pradhan, S. Biomass wastes: A potential catalyst source for biodiesel production. *Bioresour. Technol. Rep.* **2022**, *18*, 101081. [[CrossRef](#)]
10. Garcia, B.; Alves, O.; Rijo, B.; Lourinho, G.; Nobre, C. Biochar: Production, Applications, and Market Prospects in Portugal. *Environments* **2022**, *9*, 95. [[CrossRef](#)]
11. Geça, M.; Khalil, A.M.; Tang, M.; Bhakta, A.K.; Snoussi, Y.; Nowicki, P.; Wiśniewska, M.; Chehimi, M.M. Surface Treatment of Biochar—Methods, Surface Analysis and Potential Applications: A Comprehensive Review. *Surfaces* **2023**, *6*, 179–213. [[CrossRef](#)]
12. Vakros, J. Biochars and Their Use as Transesterification Catalysts for Biodiesel Production: A Short Review. *Catalysts* **2018**, *8*, 562. [[CrossRef](#)]
13. Yameen, M.Z.; AlMohamadi, H.; Naqvi, S.R.; Noor, T.; Chen, W.-H.; Amin, N.A.S. Advances in production & activation of marine macroalgae-derived biochar catalyst for sustainable biodiesel production. *Fuel* **2023**, *337*, 127215. [[CrossRef](#)]
14. Hayashi, J.; Hasegawa, I.; Hagihara, T.; Takara, T. Production of activated carbon with a large specific surface area from banana peel and its methane adsorption ability. *Carbon* **2021**, *176*, 656. [[CrossRef](#)]
15. Domingues, C.; Correia, M.J.N.; Carvalho, R.; Henriques, C.; Bordado, J.; Dias, A.P.S. Vanadium phosphate catalysts for biodiesel production from acid industrial by-products. *J. Biotechnol.* **2013**, *164*, 433–440. [[CrossRef](#)] [[PubMed](#)]
16. Foroutan, R.; Mohammadi, R.; Razeghi, J.; Ramavandi, B. Biodiesel production from edible oils using algal biochar/CaO/K<sub>2</sub>CO<sub>3</sub> as a heterogeneous and recyclable catalyst. *Renew. Energy* **2021**, *168*, 1207–1216. [[CrossRef](#)]
17. Oliveira, T.S.; Rosa, M.F.; Cavalcante, F.L.; Pereira, P.H.F.; Moates, G.K.; Wellner, N.; Mazzetto, S.E.; Waldron, K.W.; Azeredo, H.M. Optimization of pectin extraction from banana peels with citric acid by using response surface methodology. *Food Chem.* **2016**, *198*, 113–118. [[CrossRef](#)] [[PubMed](#)]
18. Acevedo, S.A.; Carrillo, J.D.; Flórez-López, E.; Grande-Tovar, C.D. Recovery of Banana Waste-Loss from Production and Processing: A Contribution to a Circular Economy. *Molecules* **2021**, *26*, 5282. [[CrossRef](#)] [[PubMed](#)]
19. Tripathy, A.; Mohanty, S.; Nayak, S.K.; Ramadoss, A. Renewable banana-peel-derived activated carbon as an inexpensive and efficient electrode material showing fascinating supercapacitive performance. *J. Environ. Chem. Eng.* **2021**, *9*, 106398. [[CrossRef](#)]
20. Sial, T.A.; Khan, M.N.; Lan, Z.; Kumbhar, F.; Ying, Z.; Zhang, J.; Sun, D.; Li, X. Contrasting effects of banana peels waste and its biochar on greenhouse gas emissions and soil biochemical properties. *Process. Saf. Environ. Prot.* **2018**, *122*, 366–377. [[CrossRef](#)]
21. Daimary, N.; Boruah, P.; Eldiehy, K.S.; Pegu, T.; Bardhan, P.; Bora, U.; Mandal, M.; Deka, D. *Musa acuminata* peel: A bioresource for bio-oil and by-product utilization as a sustainable source of renewable green catalyst for biodiesel production. *Renew. Energy* **2022**, *187*, 450–462. [[CrossRef](#)]
22. Brahma, S.; Basumatary, B.; Basumatary, S.F.; Das, B.; Brahma, S.; Rokhum, S.L.; Basumatary, S. Biodiesel production from quinary oil mixture using highly efficient *Musa chinensis* based heterogeneous catalyst. *Fuel* **2023**, *336*, 127150. [[CrossRef](#)]
23. Jitjamnong, J.; Thunyaratchatanon, C.; Luengnaruemitchai, A.; Kongrit, N.; Kasetsoomboon, N.; Sopajarn, A.; Chuaykarn, N.; Khantikulanan, N. Response surface optimization of biodiesel synthesis over a novel biochar-based heterogeneous catalyst from cultivated (*Musa sapientum*) banana peels. *Biomass Convers. Biorefinery* **2020**, *11*, 2795–2811. [[CrossRef](#)]
24. Mansoorsamaei, Z.; Mowla, D.; Esmaeilzadeh, F.; Dashtian, K. Sustainable biodiesel production from waste cooking oil using banana peel biochar-Fe<sub>2</sub>O<sub>3</sub>/Fe<sub>2</sub>K<sub>6</sub>O<sub>5</sub> magnetic catalyst. *Fuel* **2024**, *357*, 129821. [[CrossRef](#)]
25. Kumar, S.; Soomro, S.A.; Harijan, K.; Uqaili, M.A.; Kumar, L. Advancements of Biochar-Based Catalyst for Improved Production of Biodiesel: A Comprehensive Review. *Energies* **2023**, *16*, 644. [[CrossRef](#)]
26. Dias, A.P.S.; Rego, F.; Fonseca, F.; Casquilho, M.; Rosa, F.; Rodrigues, A. Catalyzed pyrolysis of SRC poplar biomass. Alkaline carbonates and zeolites catalysts. *Energy* **2019**, *183*, 1114–1122. [[CrossRef](#)]
27. Kobayashi, T.; Kuramochi, H. Optimized production conditions and activation of biochar for effective promotion of long-chain fatty acid degradation in anaerobic digestion. *Bioresour. Technol.* **2022**, *358*, 127393. [[CrossRef](#)] [[PubMed](#)]
28. Pathak, P.D.; Mandavgane, S.A.; Kulkarni, B.D. Valorization of banana peel: A biorefinery approach. *Rev. Chem. Eng.* **2016**, *32*, 651–666. [[CrossRef](#)]
29. Deokar, S.K.; Jadhav, A.R.; Pathak, P.D.; Mandavgane, S.A. Biochar from microwave pyrolysis of banana peel: Characterization and utilization for removal of benzoic and salicylic acid from aqueous solutions. *Biomass Convers. Biorefinery* **2022**, *1*, 1–12. [[CrossRef](#)]
30. Tarar, O.F.; Asghar, A.; Qayyum, S.A.; Kanwal, H.; Lateef, A.; Nazir, R.; Abidi, S.H.I.; Naeem, M.K.; Shahid, B. Synthesis and surface morphology of banana biochar-based nano-fertilizer and its effect on first stages of growth parameters of cucumber, broccoli, and red okra. *J. Saudi Soc. Agric. Sci.* **2023**, *22*, 535–545. [[CrossRef](#)]
31. Nzihou, A.; Stanmore, B.; Sharrock, P. A review of catalysts for the gasification of biomass char, with some reference to coal. *Energy* **2013**, *58*, 305–317. [[CrossRef](#)]
32. Hu, Z.-T.; Ding, Y.; Shao, Y.; Cai, L.; Jin, Z.-Y.; Liu, Z.; Zhao, J.; Li, F.; Pan, Z.; Li, X.; et al. Banana peel biochar with nanoflake-assembled structure for cross contamination treatment in water: Interaction behaviors between lead and tetracycline. *Chem. Eng. J.* **2021**, *420*, 129807. [[CrossRef](#)]

33. Ercan, B.; Alper, K.; Ucar, S.; Karagoz, S. Comparative studies of hydrochars and biochars produced from lignocellulosic biomass via hydrothermal carbonization, torrefaction and pyrolysis. *J. Energy Inst.* **2023**, *109*, 101298. [[CrossRef](#)]
34. Hussein, H.S.; Shaarawy, H.H.; Hussien, N.H.; Hawash, S.I. Preparation of nano-fertilizer blend from banana peels. *Bull. Natl. Res. Cent.* **2019**, *43*, 26. [[CrossRef](#)]
35. Meriatna; Husin, H.; Riza, M.; Faisal, M.; Ahmadi; Sulastri. Biodiesel production using waste banana peel as renewable base catalyst. *Mater. Today Proc.* **2023**, *87*, 214–217. [[CrossRef](#)]
36. Spataru, D.; Dias, A.P.S.; Ferreira, L.F.V. Acetylation of biodiesel glycerin using glycerin and glucose derived catalysts. *J. Clean. Prod.* **2021**, *297*, 126686. [[CrossRef](#)]
37. Galvão, A.C.; Jiménez, Y.P.; Justel, F.J.; Robazza, W.S.; Donatti, F.S. Salting-out precipitation of NaCl, KCl and NH<sub>4</sub>Cl in mixtures of water and methanol described by the modified Pitzer model. *J. Chem. Thermodyn.* **2020**, *150*, 106202. [[CrossRef](#)]
38. Rijo, B.; Fernando, E.; Ramos, M.; Dias, A.P.S. Biodiesel production over sodium carbonate and bicarbonate catalysts. *Fuel* **2022**, *323*, 124383. [[CrossRef](#)]
39. Dai, Y.-M.; Lin, J.-H.; Huang, S.-T.; Lee, W.-L.W.; Hsieh, C.-H.; Chen, F.-H.; Chen, C.-C. Natural soil and lithium carbonate as economical solid-base catalysts for biodiesel production. *Energy Rep.* **2020**, *6*, 2743–2750. [[CrossRef](#)]
40. Zeghioud, H.; Fryda, L.; Djelal, H.; Assadi, A.; Kane, A. A comprehensive review of biochar in removal of organic pollutants from wastewater: Characterization, toxicity, activation/functionalization and influencing treatment factors. *J. Water Process. Eng.* **2022**, *47*, 102801. [[CrossRef](#)]
41. Janu, R.; Mrlik, V.; Ribitsch, D.; Hofman, J.; Sedláček, P.; Bielská, L.; Soja, G. Biochar surface functional groups as affected by biomass feedstock, biochar composition and pyrolysis temperature. *Carbon Resour. Convers.* **2021**, *4*, 36–46. [[CrossRef](#)]
42. Wang, W.; Lemaire, R.; Bensakhria, A.; Luart, D. Review on the catalytic effects of alkali and alkaline earth metals (AAEMs) including sodium, potassium, calcium and magnesium on the pyrolysis of lignocellulosic biomass and on the co-pyrolysis of coal with biomass. *J. Anal. Appl. Pyrolysis* **2022**, *163*, 105479. [[CrossRef](#)]
43. Zafeiriou, I.; Karadendrou, K.; Ioannou, D.; Karadendrou, M.-A.; Detsi, A.; Kalderis, D.; Massas, I.; Gasparatos, D. Effects of Biochars Derived from Sewage Sludge and Olive Tree Prunings on Cu Fractionation and Mobility in Vineyard Soils over Time. *Land* **2023**, *12*, 416. [[CrossRef](#)]
44. Catarino, M.; Ferreira, E.; Dias, A.P.S.; Gomes, J. Dry washing biodiesel purification using fumed silica sorbent. *Chem. Eng. J.* **2019**, *386*, 123930. [[CrossRef](#)]
45. Jayaraju, R.M.; Gaddam, K.; Ravindiran, G.; Palani, S.; Paulraj, M.P.; Achuthan, A.; Saravanan, P.; Muniasamy, S.K. Biochar from waste bio-mass as a biocatalyst for biodiesel production: An overview. *Appl. Nanosci.* **2022**, *12*, 3665–3676. [[CrossRef](#)]
46. Wang, S.; Zhao, C.; Shan, R.; Wang, Y.; Yuan, H. A novel peat biochar supported catalyst for the transesterification reaction. *Energy Convers. Manag.* **2017**, *139*, 89–96. [[CrossRef](#)]
47. Xu, J.; Liu, J.; Zhang, X.; Ling, P.; Xu, K.; He, L.; Su, S.; Wang, Y.; Hu, S.; Xiang, J. Chemical imaging of coal in micro-scale with Raman mapping technology. *Fuel* **2020**, *264*, 116826. [[CrossRef](#)]
48. Kapteijn, F.; Abbel, G.; Moulijn, J.A. CO<sub>2</sub> gasification of carbon catalysed by alkali metals: Reactivity and mechanism. *Fuel* **1984**, *63*, 1036–1042. [[CrossRef](#)]
49. Dias, A.P.S.; Puna, J.; Gomes, J.; Correia, M.J.N.; Bordado, J.; Joana, M.; Correia, N.; Paula, A.; Dias, S.; Puna, J. Biodiesel production over lime. Catalytic contributions of bulk phases and surface Ca species formed during reaction. *Renew. Energy* **2016**, *99*, 622–630. [[CrossRef](#)]
50. Catarino, M.; Martins, S.; Dias, A.P.S.; Pereira, M.F.C.; Gomes, J. Calcium diglyceroxide as a catalyst for biodiesel production. *J. Environ. Chem. Eng.* **2019**, *7*, 103099. [[CrossRef](#)]
51. Rijo, B.; Dias, A.P.S.; Carvalho, J.P.S. Recovery of carbon fibers from aviation epoxy composites by acid solvolysis. *Sustain. Mater. Technol.* **2023**, *35*, 14–16. [[CrossRef](#)]
52. Wang, X.; Chen, Q.; Zhu, H.; Chen, X.; Yu, G. In-situ study on structure evolution and gasification reactivity of biomass char with K and Ca catalysts at carbon dioxide atmosphere. *Carbon Resour. Convers.* **2023**, *6*, 27–33. [[CrossRef](#)]

**Disclaimer/Publisher’s Note:** The statements, opinions and data contained in all publications are solely those of the individual author(s) and contributor(s) and not of MDPI and/or the editor(s). MDPI and/or the editor(s) disclaim responsibility for any injury to people or property resulting from any ideas, methods, instructions or products referred to in the content.